14 (2022) 200244

Contents lists available at ScienceDirect

Tumour Virus Research

journal homepage: www.journals.elsevier.com/tumour-virus-research

Synergistic targeting of the PI3K/mTOR and MAPK/ERK pathways in Merkel cell carcinoma

Arturo Temblador [a], Dimitrios Topalis [a], Graciela Andrei [a,*], Robert Snoeck [a]

[a] Rega Institute for Medical Research, Department of Microbiology, Immunology and Transplantation, Laboratory of Virology and Chemotherapy, KU Leuven, 3000, Leuven, Belgium

ARTICLE INFO

Keywords:
Merkel cell carcinoma
Merkel cell polyomavirus
Synergism
Combined targeting
Pathway inhibition

ABSTRACT

Merkel cell carcinoma (MCC) is an aggressive type of skin cancer, which is caused either by integration of the oncogenic Merkel cell polyomavirus (MCPyV) or by accumulation of UV-light induced mutations. Since the response to immune-checkpoint inhibitors is limited, new therapeutic agents need to be explored. Previous studies have shown that MCC cell lines and xenografts are sensitive to MLN0128, a dual mTOR1/2 inhibitor. Prompted by these results and considering that the PI3K/mTOR and MAPK/ERK pathways are the most commonly deregulated pathways in cancer, the combination of MLN0128 with the MEK1/2 inhibitor trametinib was investigated. Importantly, the combined targeting showed to be synergistic in MCC cell lines and induced alterations in the protein levels of downstream elements of the targeted pathways. This synergistic activity implies a reduction in the dose of each inhibitor necessary to reach the same effect that when used as single agents. Therefore, this is a promising approach to improve the clinical management of MCC and to overcome the limited efficacy of single drug regimens owed to the appearance of toxicity or drug resistance.

1. Introduction

Merkel cell carcinoma (MCC) is a rare type of skin cancer with two recognized aetiologies. In 2008, a new human polyomavirus, i.e. Merkel cell polyomavirus (MCPyV), was identified clonally integrated in ~80% of MCCs [1]. Tumorigenesis of MCPyV-positive ($MCPyV^+$) MCC is driven by the constitutive expression of two viral oncoproteins, the small (sT) and large (LT) tumor antigens (TAs), which maintain cell growth by blocking retinoblastoma (Rb) function [2–4], among other mechanisms [5]. Conversely, MCPyV-negative ($MCPyV^-$) MCCs arise upon accumulation of mutations with an UV-light signature [6].

MCC usually appears in sun-exposed areas of elderly fair-skinned individuals, with a median age at diagnosis of 69 years, with 90% of the patients over 50 years [7]. The incidence is higher among immunosuppressed individuals [8] and it varies greatly geographically, being greater in North America (0.7 cases/100,000 individuals), Europe (around 0.59) and particularly, Australia and New Zealand (1.6 and 0.96, respectively) [9–11]. These last two countries have a predominant population of Caucasian origin exposed to a large UV-light index, which may explain why the virus-negative MCC is more common [10,12].

MCC is an aggressive cancer with a 5-year relative survival of only 18% in patients presented with metastatic disease [13]. Since MCC is an immunogenic tumor [12], it responds well to immune-checkpoint inhibitors, such as avelumab and pembrolizumab. Therefore, the Food and Drug Administration (FDA) has approved these two drugs as preferable treatment for patients with metastatic MCC [14]. Nevertheless, some patients never respond, and others develop resistance to the treatment. Consequently, new therapeutic approaches continue to be investigated [12].

Despite presenting different aetiologies, the two MCC subtypes share common deregulated pathways, such as inactivation of Rb [5,15]. Similarly, the phosphatidylinositol 3-kinase/mammalian target of rapamycin (PI3K/mTOR) pathway is often activated in MCC, although only a subset of tumors presented activating mutations [16–19]. Consequently, MCC cell lines and xenografts are sensitive to mTOR inhibitors [20]. The PI3K/mTOR and the mitogen-activated protein

Abbreviations: $MCPyV^+$, Merkel cell polyomavirus-positive;; $MCPyV^-$, Merkel cell polyomavirus-negative;; MCC, Merkel cell carcinoma;; sT, small T antigen;; LT, large T antigen;; TAs, tumor antigens;; Rb, retinoblastoma;; PI3K/mTOR), phosphatidylinositol 3-kinase/mammalian target of rapamycin;; FDA, Food and Drug Administration;; MAPK/ERK, mitogen-activated protein kinase/extracellular-signal-regulated kinase;; mTORC1/2, mammalian target of rapamycin complex 1/2 or mechanistic target of rapamycin complex 1/2;.

* Corresponding author. Rega Institute For Medical Research, Herestraat 49, postbus 1030, 3000, Leuven, Belgium.
E-mail address: graciela.andrei@kuleuven.be (G. Andrei).

https://doi.org/10.1016/j.tvr.2022.200244
Received 4 October 2021; Received in revised form 27 January 2022; Accepted 8 August 2022
Available online 22 August 2022

kinase/extracellular-signal-regulated kinase (MAPK/ERK) pathways control cell proliferation, apoptosis, protein translation and glycolytic metabolism. Therefore, they are central players in cancer progression, and a crosstalk exists between them (Fig. 1) [21,22]. mTOR presents two different complexes: mTORC1, which is directly involved in regulation of mRNA translation through the phosphorylation of eIF4E-binding proteins (4E-BPs), and mTORC2, that controls cell survival through Akt activity [23]. Tuberous sclerosis complex (TSC) is a negative regulator of mTORC1 that can be inactivated by Akt and by downstream substrates of the MAPK/ERK pathway, affecting mRNA translation [22]. In addition, MCPyV sT has been shown to reduce the turnover of hyperphosphorylated 4E-BP1, increasing cap-dependent translation [24].

Inhibitors of PI3K/mTOR may upregulate tyrosine kinase receptors (TKRs), cytoplasmic kinases (RSK), anti-apoptotic proteins (Bcl-2), and transcription factors (FOXO), giving rise to acquired resistance [25]. Moreover, these changes may lead to activation of compensatory pathways, limiting the efficacy of targeted drugs. For instance, mTORC1 inhibition has been shown to activate the MAPK/ERK pathway through S6K-PI3K-Ras signalling [26]. Nevertheless, combination of inhibitors of related pathways has proved to enhance the growth inhibitory effects *in vitro* and *in vivo* [26,27]. These findings provide a rationale for a combined targeting in order to avoid compensatory re-activation of the pathway not inhibited when using single agents. A recent publication described that activation of the JAK2 and MEK-ERK pathways was more important in MCPyV$^-$ MCC cell lines than in MCPyV$^+$ MCC cell lines, suggesting that the JAK-STAT and MEK-ERK signalling pathways may be potential targets for therapy of MCPyV$^-$ MCC [28]. MLN0128, a second-generation dual TORC1/2 inhibitor, significantly diminished the growth of MCC xenografts in mice independently of MCPyV [20]. Further, MLN0128 robustly hampered MCC cell proliferation and induced apoptosis whereas senescence did not contribute to drug-mediated growth inhibition of MCC xenografts. Marked antitumor effects of MLN0128 were as well found when the drug was administered in combination therapy with the bromodomain protein BRD4 inhibitor JQ1, suggesting that dual targeting of PI3K/mTOR pathway and c-Myc axis is efficient in the restraining MCC tumor growth [20]. Considering that the MAPK/ERK pathway has been reported to be activated in MCC, the sensitivity of MCC to mTOR inhibitors, the efficacy of MLN0128 in combination therapy with JQ1, and the crosstalk between these pathways, PI3K/mTOR and MAPK/ERK pathways should be explored as relevant targets for a combined MCC therapy. Therefore, we investigated the synergistic activity of MLN0128 (sapanisertib), an ATP-competitive $mTOR_{1/2}$ serine/threonine kinase inhibitor, and trametinib, a MEK1/2 tyrosine kinase inhibitor (Fig. 1). The former showed good activity against MCC [20] and is currently under clinical investigation (NCT02514824) while the latter is used in combination with dabrafenib (a BRAF inhibitor) for the treatment of patients with $BRAF_{V600E/K}$-mutant metastatic melanoma [29,30].

Our results showed that this drug combination is synergistic across a panel of MCC cell lines. To gain insight into the molecular mechanisms involved in the antiproliferative effects of these compounds, alterations in the expression levels of key substrates of the targeted pathways were analyzed by Western blot. Additionally, the cell cycle phase distribution of treated cells was determined by propidium iodide (PI) staining of cell nuclei.

2. Materials & methods

2.1. Cell lines

WAGA cell line was kindly provided by Roland Houben (University Hospital Würzburg, Germany). The rest of the cell lines used in the present study were obtained from the European Collection of Authenticated Cell Cultures (ECACC): MCC13 (Cat#10092302), MCC14/2 (Cat#10092303), MCC26 (Cat# 10092304), MS-1 (Cat#09111802) and MKL-1 (Cat#09111801). MCPyV$^-$ MCC cell lines (MCC13, MCC14/2 and MCC26) were grown in RPMI 1640 medium supplemented with 10% FBS. MCPyV$^+$ MCC cell lines (MS-1, MKL-1 and WAGA) were maintained in RPMI 1640 + GlutaMAX™-I medium supplemented with 20% FBS. Media were supplemented with 1x MEM NEAA, 1 mM sodium pyruvate, 1x Penicillin/Streptomycin/Glutamine and 10 mM HEPES. All

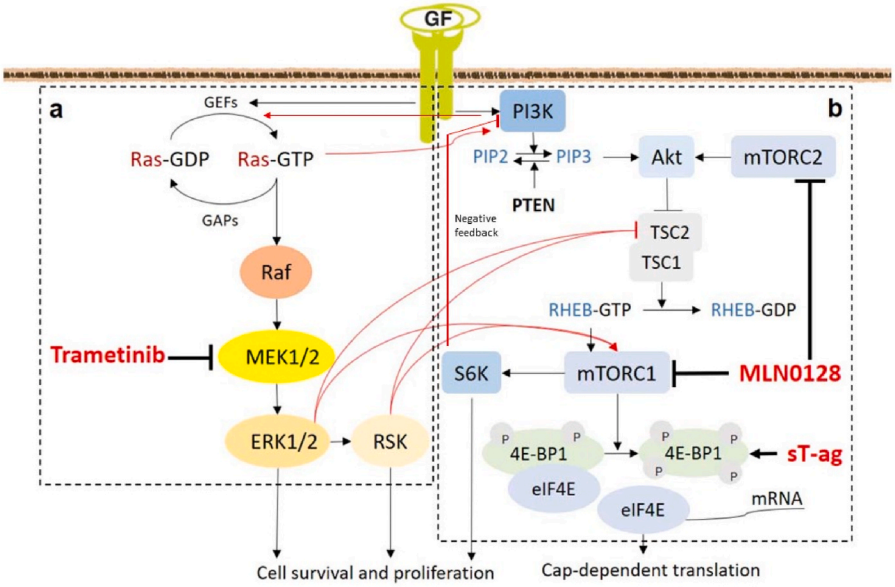

Fig. 1. MAPK and PI3K/mTOR pathways, crosstalk and targeting. (**a**) Activated GEFs proteins catalyze Ras-GTP exchange and lead to the activation of Raf, which causes a phosphorylation cascade that ultimately will activate ERK1/2 and RSK. (**b**) PI3K generates PIP3, which recruits Akt and then it is activated by mTORC2. PTEN acts as a negative regulator of PI3K. Akt promotes the activation of mTORC1, which in turn phosphorylates 4E-BP1 and S6K. Phosphorylation of 4E-BP1 inhibits its ability to bind eIF4E mRNA cap-binding protein. MCPyV sT-ag maintains the hyperphosphorylated state of 4E-BP1. TSC is a regulator of mTORC1, and it functions as a guanosine triphosphatase-activating protein for the small guanine nucleotide-binding protein Rheb. The activation of A and B leads to increased cell survival and proliferation, activation of glycolytic metabolism and protein translation. The arrows in red indicate cross-activation mechanisms. Positive regulation of the substrate is indicated by an arrow, while negative regulation is depicted as a blunt-ended line. The targets of trametinib and MLN0128 are indicated. **Abbreviations:** GF, growth factor; GEFs, guanine-nucleotide exchange factors; GAPs, GTPase-activating proteins; Ras, rat sarcoma; Raf, rapidly growing fibrosarcomas; MEK1/2, MAP kinase; ERK1/2, extracellular signal-regulated kinase; RSK, p90 ribosomal S6 kinase; PI3K, phosphatidylinositol 3-kinase; PIP2, phosphatidylinositol 4,5-bisphosphate; PIP3, phosphatidylinositol 3,4,5 triphosphate; PTEN, phosphatase and tensin homolog; $TSC_{1/2}$, tuberous sclerosis complex; mTORC1/2, mammalian target of rapamycin complex; RHEB, Ras homolog enriched in brain; S6K, p70 ribosomal S6 kinase; 4E-BP1, eIF4E-binding protein 1; eIF4E, eukaryotic initiation factor 4E. (For interpretation of the references to colour in this figure legend, the reader is referred to the Web version of this article.)

media and supplements were purchased at Thermo Fisher Scientific (Merelbeke, Belgium).

2.2. Determination of antiproliferative activity of MLN0128 and trametinib

10,000 (MCPyV$^-$) or 20,000 (MCPyV$^+$) cells per well were seeded in 96-well plates and counted every other day, for eight days, to build a cell growth curve. Then, the same cell number was seeded in 96-well plates and one day after serial dilutions of MLN0128 or trametinib were added in duplicate to cells. After six days of incubation at 37 °C with 5% CO_2, cells growing in exponential phase were counted with a Beckman Z1 Coulter Counter. Prior to counting, cell clusters of MS-1 and MKL-1 were disrupted using EDTA. The antiproliferative effects were expressed as the compound concentration needed to inhibit cell growth by 50% (CC_{50}).

2.3. Determination of synergistic activity

MCC cells were seeded in 96-well plates as described above. Subsequently, cells were incubated with serial dilutions of trametinib and MLN0128, alone or in combination, comprising concentrations above and below their respective CC_{50} for each cell line (see Supplementary Table S1). A coulter counter system was used to determine the fraction of cells affected at each given drug-dose. These values were introduced in the Compusyn software (ComboSyn, Inc.) to construct dose-effect curves. The dose-effect curves were generated using four to eight data points for each drug alone and five or six data points for the combinations. A different combination ratio was used for each cell line, according to the values of their respective CC_{50} for each compound. The Compusyn software utilizes the method developed by Chou-Talalay to calculate a combination index (CI) [31,32]. The CI provides a value indicating the extension of the synergism for a given drug combination: $CI < 1$, $= 1$, and >1 indicate synergism, additive effect and antagonism, respectively. Additionally, the dose reduction index (DRI), which is obtained by dividing the dose of a drug when used alone by the dose of the same drug in the combination necessary to achieve the same effect, was calculated. Thus, a DRI>1 indicates a favourable dose reduction [33].

2.4. Protein extraction and immunoblotting

Protein extracts were obtained after six days of incubation with each drug alone or in combination. For this purpose, RIPA Buffer (Thermo Fisher Scientific) containing cOmplete™, Mini, EDTA-free Protease Inhibitor Cocktail (Roche Applied Science) and Phosphatase Inhibitor Cocktail (Active Motive) was used. Protein concentration was determined with a BCA assay (Thermo Fisher Scientific). Then, proteins were separated by SDS-PAGE on precast gels (Bio-Rad Laboratories, Hercules, CA, USA), transferred to PVDF membranes and incubated overnight at 4ºC with the correspondent primary antibody. Next day, membranes were incubated with HRP-conjugated secondary antibodies for 1 h at room temperature. Peroxidase activity was detected using the Super-Signal™ West Femto Maximum Sensitivity Substrate (Bio-Rad). Images were captured with a ChemiDoc™ MP Imaging System and analyzed with Image Lab™ v6 software (Bio-Rad). ImageJ was used for densitometry analysis. The following antibodies were used: anti-actin [ACTN05 (C4)] (Cat# ab3280) from Abcam (Cambridge, UK); anti-4E-BP1 (53H11) (Cat#9644), anti-Phospho-4E-BP1 (Ser65) (Cat#9451), anti-p44/42 MAPK (ERK1/2) (Cat#9102) and anti-Phospho-p44/42 MAPK (ERK1/2) (Thr202/Tyr204) (Cat#9101) from Cell Signalling Technology (Danvers, MA, USA).

2.5. Cell cycle analysis

Upon 24 h incubation with single and combined agents, BD Cycletest™ Plus DNA Kit (BD Biosciences) was used to stain cellular nuclei with propidium iodide (PI), following the manufacturer's instructions. Cell cycle phase distribution was evaluated using BD FACS-Celesta flow cytometer. Data were analyzed with FlowJo v10 (Tree Star, Williamson Way, Ashland, OR).

2.6. Statistics

Drug combination experiments were repeated at least three times to calculate the mean ± SD values of each parameter. One-way ANOVA tests were performed for statistical analysis using GraphPad Prism 7 (GraphPad Software Inc., La Jolla, CA). Tukey test was used to correct *P*-value when comparing the different treatment groups. Significance was defined with the following *P*-values: $^*P < 0.05$, $^{**}P < 0.01$ and $^{***}P < 0.001$.

3. Results

3.1. The combination of trametinib and MLN0128 is synergistic in MCC cell lines

Initially, the growth curve of each cell line was drawn (see Supplementary Fig. S1) to determine the time required to reach exponential growth. Then, dose-response experiments with each drug alone were performed to determine their respective CC_{50} value in three virus-negative (MCC13, MCC14/2 and MCC26) and three virus-positive (MS-1, MKL-1 and WAGA) MCC cell lines. Fig. 2A shows the CC_{50} of each drug for all the MCC cell lines used in this study. Trametinib exhibited a CC_{50} lower than 0.5 μM for the virus-negative cell lines. On the contrary, it ranged between 10 and 20 μM for the virus-positive cells. MLN0128 displayed a CC_{50} lower than 0.2 μM for all cell lines, with the exception of MS-1.

The synergistic activity between the two drugs was explored using the method designed by Chou and Talalay, who developed a parameter called combination index (CI), indicating the extension of the synergism for a given level of cytostaticity [33]. As shown in Fig. 2B, the combination of trametinib and MLN0128 was synergistic ($CI < 1$) in all the MCC cell lines for a cytostatic effect of 50% and 75%, except for MS-1 and MKL-1 at 75% and 50% of cytostaticity, respectively. Supplementary Fig. S2 shows representative dose-effect curves for each drug alone and for the combination in each cell line, as well as the median-effect plot, which is a linearized form of all dose-effect curves. These plots were generated by the Compusyn software.

3.2. Reduced concentration of each compound is required for the combined targeting

As represented in Fig. 3A, the dose reduction index (DRI) for each compound (trametinib or MLN0128) was higher than 1 when their combination induced cytostaticity effect of 50% and 75% in MCC cell lines, indicating a favourable dose reduction in these cases. Indeed, lower concentrations of each compound were used in the combination to reach the same level of cytostaticity (Fig. 3B). Considering the drug ratios used in the combination, the individual CC_{50} values of each compound when used together were calculated (summarized in Table 1). This fold-change in the CC_{50} corresponded with the value expressed by the DRI.

3.3. Altered protein levels of downstream elements of the MAPK and PI3K/mTOR pathways upon incubation with drugs

Total protein and phosphorylated form (P-) of 4E-BP1, an effector of the PI3K/mTOR pathway, and ERK1/2, a downstream effector of the MAPK pathway, were analyzed by Western blot to address the effects of the inhibition of these pathways by single drugs and their combination. Each cell line was incubated with concentrations of trametinib and

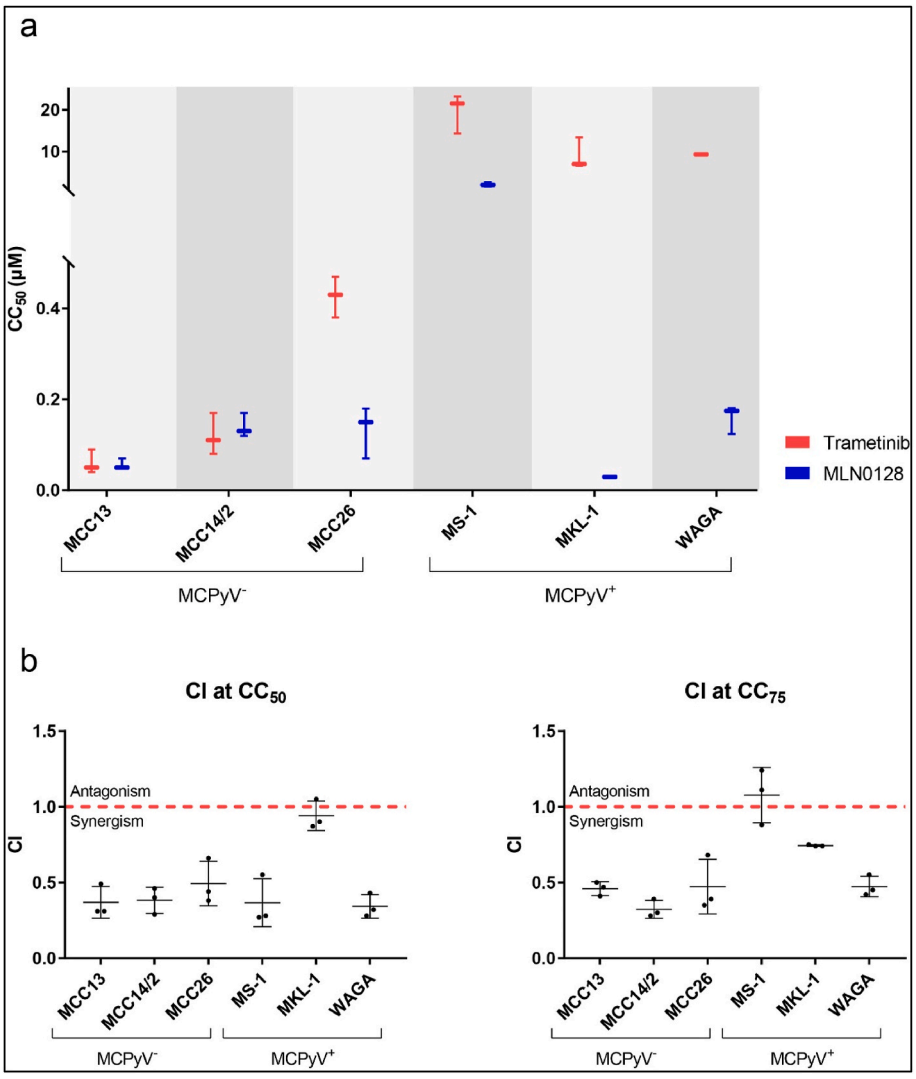

Fig. 2. Combined targeting with trametinib and MLN0128 in MCC cell lines. (**a**) CC_{50} of trametinib (red) and MLN0128 (blue) in three virus-negative and three virus-positive MCC cell lines. (**b**) CI at 50% and 75% of cytostatic effect for the same cell lines. CI < 1 indicates synergism. Data represent the mean ± SD of three independent experiments (n = 3). (For interpretation of the references to colour in this figure legend, the reader is referred to the Web version of this article.)

MLN0128 comprising their respective CC_{50} alone or in combination, as indicated in Table 1. As seen in Fig. 4A, virus-negative cell lines tended to decrease total 4E-BP1 protein when treated with the mTOR1/2 inhibitor (MLN0128) or with its combination with trametinib, with around 2-fold reduction in MCC13 and MCC14/2. This decrease was more significant for the combined targeting. Regarding P- 4E-BP1 level, there was a marked increase in those virus-negative cells treated with trametinib or with its combination with MLN0128 when compared with untreated cells. When cells were treated only with MLN0128, which is expected to dephosphorylate 4E-BP1 via the inhibition of mTORC1, the levels of P-4E-BP1 were comparable to those of the control or even considerably lower, e.g. for MCC26. In the case of the virus-positive cell lines, total 4E-BP1 slightly increased in cells treated with the two compounds alone or in combination, though significant differences were only observed in WAGA cells (Fig. 4B). Nevertheless, P-4E-BP1 was significantly decreased in those virus-positive cells treated with both MLN1028 alone and combined with trametinib. The p44/42 MAPK antibody detects two isoforms, the middle band correspond to the 44-kDa isoform (p44 or ERK1) while the lower one is the 42-kDa isoform (p42 or ERK2). However, a third upper band was also detected in our experiments. Generally, there were not significant differences in the total amount of p42 and p44 in both virus-negative and positive cells under the different conditions. The phosphorylated forms of p42 and p44 were slightly decreased in virus-negative cells treated with trametinib, alone or in combination with MLN0128, yet significant results were not only obtained. Surprisingly, virus-positive cells had a significant reduction of P-p42 and P-p44 when treated with trametinib alone and when combined with MLN0128.

3.4. Cell cycle analysis

The cell cycle phase distribution of cells treated with each compound alone or in combination was analyzed by PI staining of cell nuclei at day 1 post-treatment (Fig. 5). However, a significant difference was only observed in the S phase of MCC13 cells treated with the two compounds alone and in combination.

4. Discussion

MCC is a rare type of skin cancer yet the incidence is increasing exponentially [9,34]. The high mortality rate associated with this disease (33–46%) makes it one of the most aggressive types of skin cancer [12]. Despite the success of immunotherapies, 40%–60% of cases do not respond [35,36]. Herein, we investigated the combined targeting of the

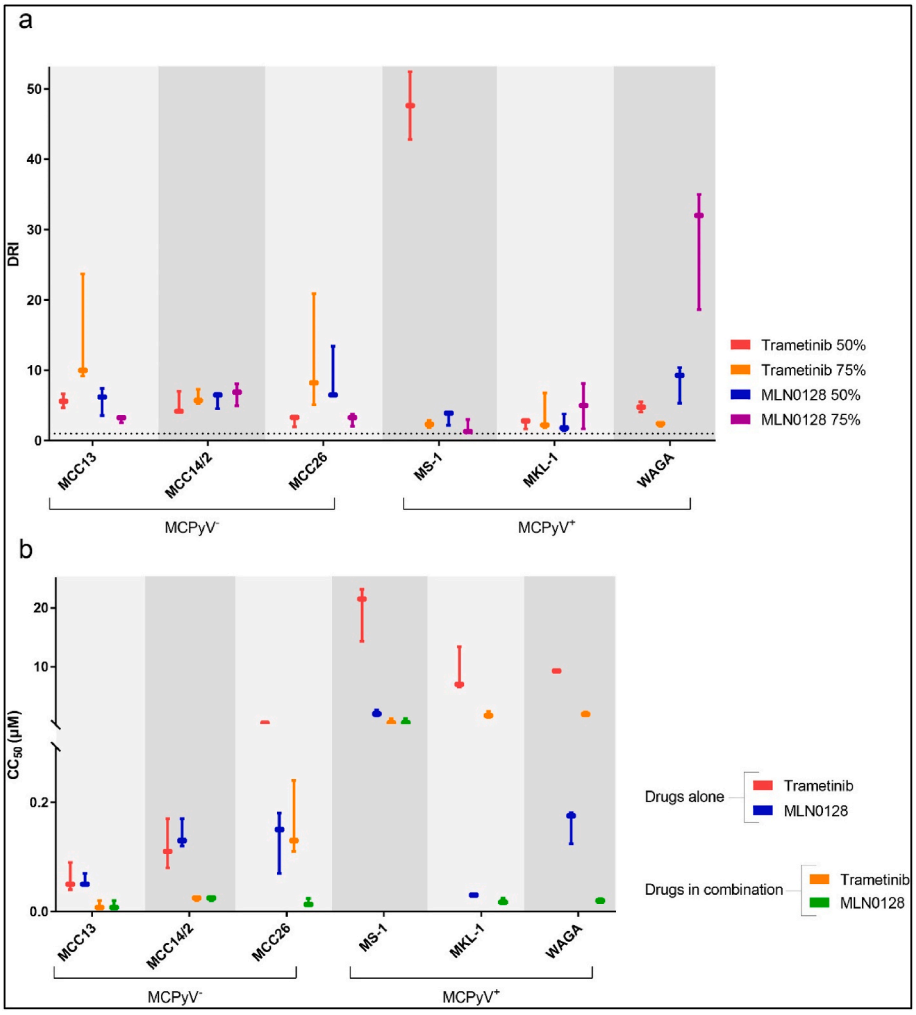

Fig. 3. Reduction of the concentration of each compound in the combined targeting. (**a**) Dose reduction index (DRI) of each compound at two different cytostatic effect for three virus-negative cell lines and three virus-positive cell lines. Dotted line indicates a DRI value of 1. DRI was calculated by dividing the dose of a drug when used alone by the dose of the same drug in the combination necessary to achieve the same effect. (**b**) Comparison between the CC_{50} of each drug when used alone and when used combined. Data represent the mean ± SD of three independent experiments (n = 3).

Table 1
CC_{50} values of trametinib and MLN0128 alone or in combination. Data represent the mean ± SD of three independent experiments (n = 3).

Cell line	CC_{50} Trametinib (μM)	CC_{50} MLN0128 (μM)	Ratio combination	CC_{50} Combination (μM)	CC_{50} Trametinib in Combination (μM)	CC_{50} MLN0128 in Combination (μM)
MCC13	0.06 ± 0.026	0.056 ± 0.011	1:1	0.023 ± 0.015	0.0115	0.0115
MCC14/2	0.12 ± 0.046	0.14 ± 0.026	1:1	0.046 ± 0.005	0.023	0.023
MCC26	0.42 ± 0.045	0.13 ± 0.057	10:1	0.17 ± 0.075	0.153	0.017
MS-1	19.66 ± 4.68	2.14 ± 0.48	1:1	1.45 ± 0.87	0.725	0.725
MKL-1	9 ± 3.81	0.03 ± 0.001	100:1	2.12 ± 0.35	2.1	0.0212
WAGA	9.34 ± 0.1	0.16 ± 0.03	100:1	2 ± 0.33	1.98	0.02

PI3K/mTOR and MAPK/ERK pathways, two cellular pathways essential for cancer progression, as a new approach for the treatment of patients with MCC.

First, the antiproliferative potential of two single drugs, trametinib and MLN0128, was determined. Trametinib was more potent in reducing cell proliferation in the virus-negative cells than in the virus-positive ones. In general, MLN0128 inhibited cell growth at the same extent in all the cell lines tested, except MS-1. The Chou-Talalay method was applied to determine the synergistic activity between the two drugs. Synergy was investigated at 50% and 75% of cytostaticity, since targeting a large number of cells is more relevant for cancer therapy. The CI values indicated synergism in the MCC cell lines analyzed. In addition, the DRI values showed favourable reduction of the dose of each drug when used together while maintaining the same efficacy. Hence, the combined treatment would be more effective in suppressing cell growth with several folds of drug reduction when compared with single treatments.

The Chou-Talalay method to determine the synergism is mechanism-independent and each drug can have several modes of action contributing to the synergy at different extents [33]. Nevertheless, we analyzed by Western blot the total protein levels and the phosphorylated forms of two downstream elements of the targeted pathways: 4E-BP1 and ERK1/2. In the virus-negative cell line MCCC13, decreased total levels of 4E-BP1 were found when treated with either inhibitor alone or combined (Fig. 4). Reduced total levels of 4E-BP1 were only found for the two other MCPyV- cells when treated with Trametinib alone or in combination with MLN0128 (MCC14/2) or only in combination with both drugs (MCC26). In contrast, total levels of 4E-BP1 did not change in the virus-positive cells except for WAGA, which experienced an increase. Targeting of mTOR with MLN0128 is expected to dephosphorylate

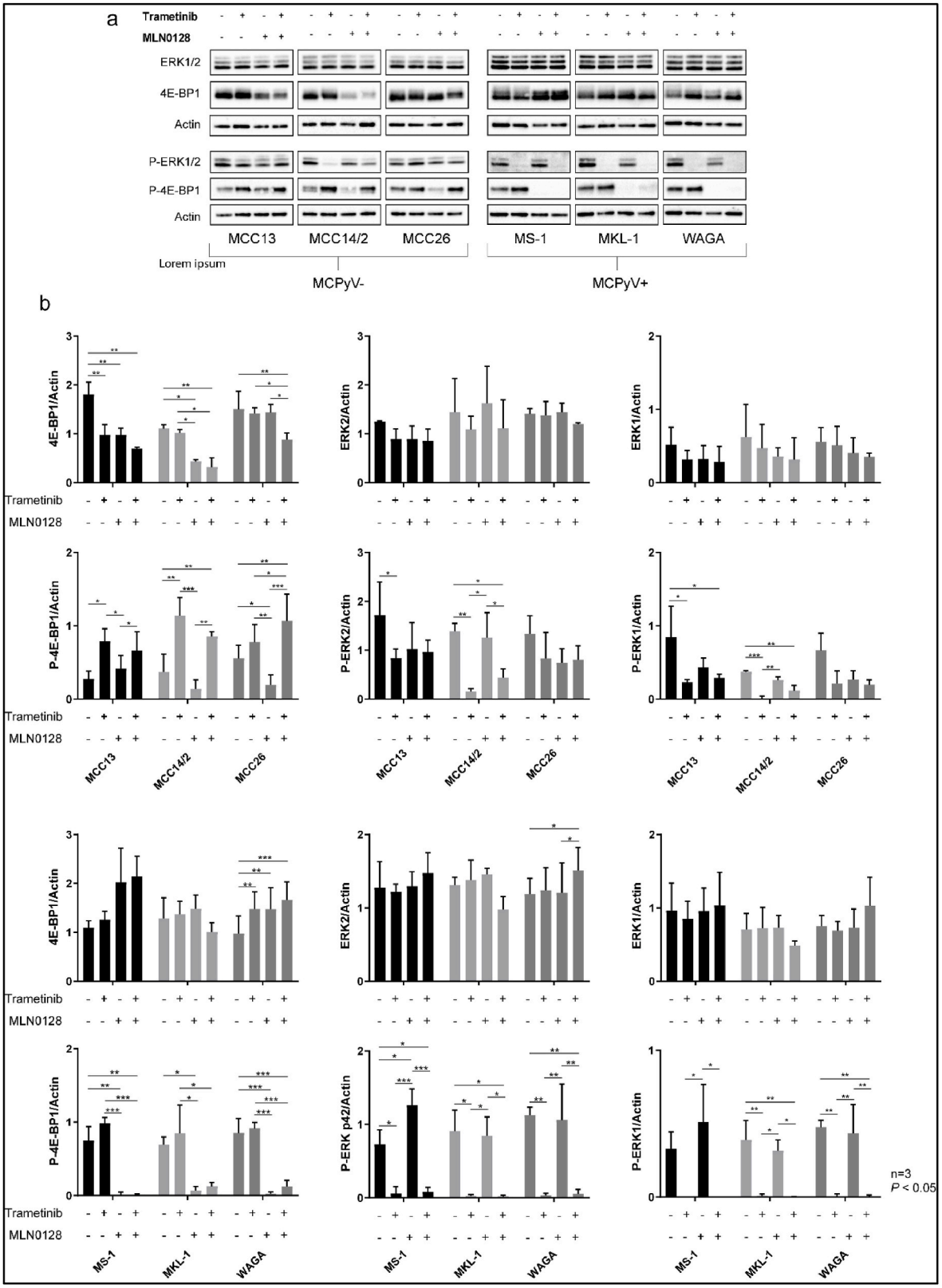

Fig. 4. Altered protein levels of downstream elements of the PI3K/mTOR and MAPK/ERK pathways in MCC cell lines upon incubation with drugs. (**a**) Each cell line was incubated with trametinib and MLN0128 alone or in combination, as indicated on top of the blots. Protein extracts were obtained after six days of drug incubation. For each cell line, representative western blots of at least three independent experiments are shown. Actin was used as internal loading control. (**b**) The plots depict the densitometry analysis of proteins normalized to actin. Data represent mean values ± SD of three independent blots. Statistical significance ($P < 0.05$) is indicated.

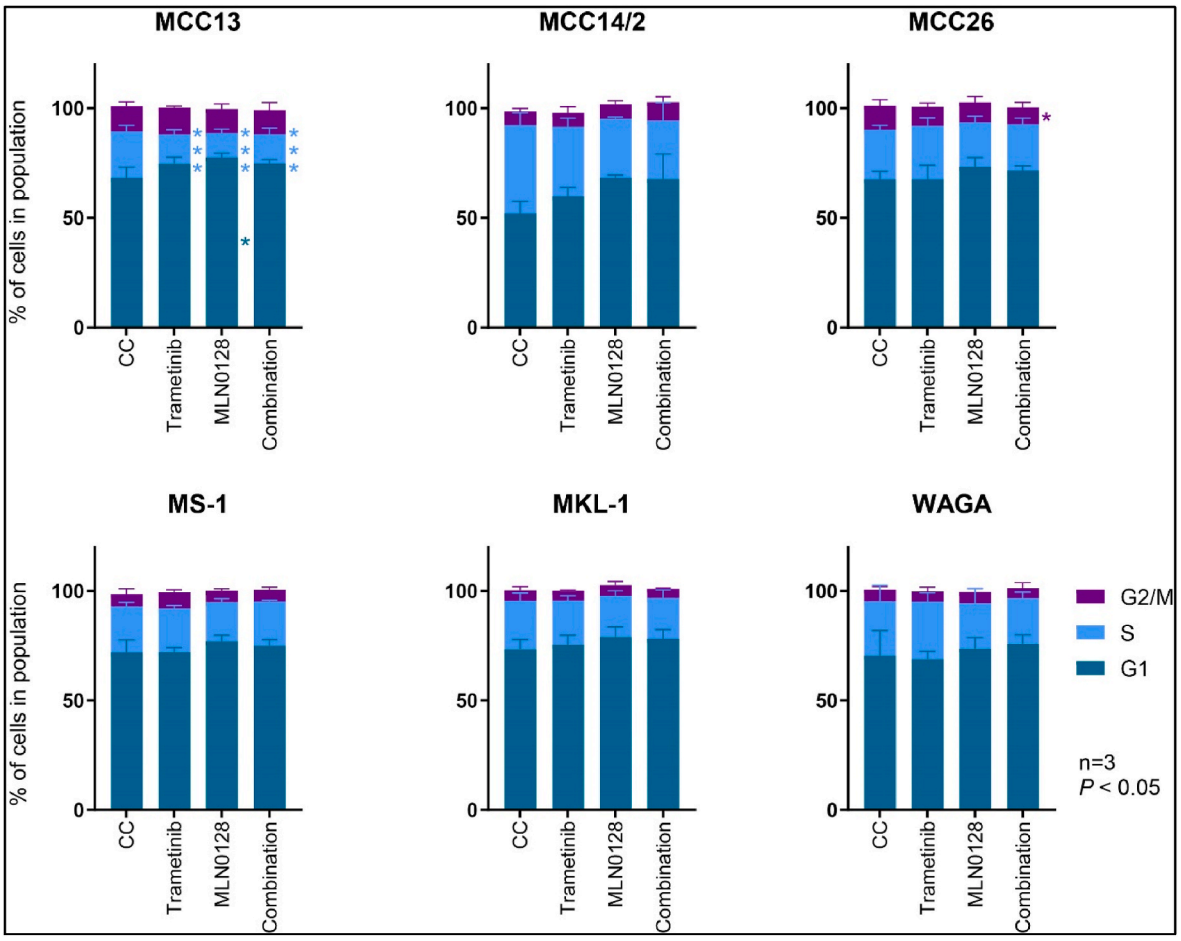

Fig. 5. Cell cycle distribution of MCC cells incubated with trametinib and MLN0128 individually and in combination. One day after adding the compounds, cell nuclei were stained with PI to analyze cell cycle distribution. The plots depict the percentage of cells in each phase of the cell cycle. Data represent mean values ± SD of three independent blots. Statistical significance ($P < 0.05$) is indicated.

4E-BP1. However, the levels of P-4E-BP1 significantly increased in the virus-negative cells treated with trametinib alone and concurrently with MLN0128, suggesting that the PI3K/mTOR pathway could act as a salvage route to the inhibition of the MAPK/ERK pathway in these cells. On the contrary, when the virus-negative cells were treated with MLN0128 alone, P-4E-BP1 tended to decrease (MCC26) or to maintain the levels of the untreated cells (MCC13 and MCC14/2). The virus-positive cells showed a marked decrease in the levels of P-4E-BP1 upon incubation with MLN0128 alone or when combined with trametinib. Generally, the levels of total ERK1/2 (or p44/p42) were invariable in virus-negative and positive cells upon treatment with the compounds alone and in combination. As expected, after treating with trametinib alone and combined with MLN0128, the levels of the phosphorylated forms were decreased, especially in the virus-positive cells. Hence, differences in cell signalling were observed regarding the viral status of the cells. Generally, the decrease of the activated forms of each element (4E-BP1 or ERK1/2) was more significant for the virus-positive cells. A synergistic pathway regulation in MCPyV$^-$ cells cannot be claimed. It can be hypothesized that due to the higher mutational burden in the virus-negative tumors, MCPyV$^-$ MCC cells may activate complementary pathways that bypass the effects of the inhibitory drugs, as previously reported [25,27,37,38].

In general, the cell cycle progression of MCC cell lines (except MCC13) was not significantly impaired upon inhibition of the PI3K/mTOR and MAPK/ERK pathways. Thus, our results suggest that the cytostatic effects observed upon single and combined targeting may not be due to alterations in the cell cycle. Nevertheless, MCC cells are characterized by a slow growth [39], presenting a prominent peak in G1 phase, especially in the case of the virus-positive cells. This makes it complicated to demonstrate a cell cycle arrest in this type of cells.

The emergence of acquired resistance associated with targeted monotherapy prompts the development of novel approaches to treat cancer. Resistance is often due to intra tumor heterogeneity where a drug may eliminate cells with certain alterations, but those with activated alternative oncogenic pathways might survive. This can be prevented with the simultaneous inhibition of multiple pathways, which can also overcome compensatory activation between related pathways. Moreover, combination therapy reduces the toxicity associated with higher doses of single agents [37,38].

Our results showed that dual inhibition of the PI3K/mTOR and MAPK/ERK pathways may be a potent therapeutic strategy for MCC. To the best of our knowledge, the efficacy of the combined therapy with agents targeting these pathways has not been explored for MCC yet. Due to suboptimal dosing schedules, this approach has shown limited long-term tolerability in clinical trials with other types of solid tumors [40]. Future research should focus on the specificity of MLMN0128 and trametinib on MCC cell lines and their possible therapeutic use. This drug combination should be evaluated in xenografts of MCC tumor cells and/or on non-tumor cells such as keratinocytes or dermal fibroblasts. Nevertheless, there are numerous studies ongoing that are expected to deliver promising results (e.g., NCT03433183).

Owing the genetic diversity of MCC tumors, we believe that combination therapies with drugs having different modes of action is a reasonable approach to investigate new treatment options. Further

experiments should be focused on testing the efficacy and selectivity of our combined targeting *ex vivo* and *in vivo* models of MCC. In addition, multiple combinations of targeted therapies together with immunotherapies, chemotherapy and radiotherapy is a promising strategy that still need clinical validation for MCC [41].

Ethics approval and consent to participate

Not applicable.

Consent for publication

Not applicable.

Availability of data and materials

The datasets used and/or analyzed during the current study are available from the corresponding author on reasonable request. All data generated or analyzed during this study are included in this published article [and its supplementary information files].

Funding

This research was supported by KU Leuven.

Authors' contributions

Conceptualization, A.T., D.T., G.A. and R.S.; Validation, Formal Analysis, Investigation, Writing – Original Draft and Visualization, A.T.; Writing – Review & Editing and Supervision, D.T., G.A. and R.S.

Authors statement

The work described in this manuscript has not been published previously (except in the form of an academic thesis), is not under consideration for publication elsewhere, is approved by all authors and tacitly or explicitly by the responsible authorities where the work was carried out, and, if accepted, it will not be published elsewhere in the same form, in English or in any other language, including electronically without the written consent of the copyright-holder.

Declaration of competing interest

The authors declare that they have no known competing financial interests or personal relationships that could have appeared to influence the work reported in this paper.

Acknowledgements

We acknowledge Professor Roland Houben for providing the WaGa cells.

Appendix A. Supplementary data

Supplementary data to this article can be found online at https://doi.org/10.1016/j.tvr.2022.200244.

References

[1] H.C. Feng, M. Shuda, Y. Chang, P.S. Moore, Clonal integration of a polyomavirus in human Merkel cell carcinoma, Science 319 (5866) (2008) 1096–1100.
[2] R. Houben, C. Adam, A. Baeurle, S. Hesbacher, J. Grimm, S. Angermeyer, K. Henzel, S. Hauser, R. Elling, E.-B. Brocker, S. Gaubatz, J.C. Becker, D. Schrama, An intact retinoblastoma protein-binding site in Merkel cell polyomavirus large T antigen is required for promoting growth of Merkel cell carcinoma cells, Int. J. Cancer 130 (4) (2012) 847–856.
[3] R. Houben, S. Angermeyer, S. Haferkamp, A. Aue, M. Goebeler, D. Schrama, S. Hesbacher, Characterization of functional domains in the Merkel cell polyoma virus Large T antigen, Int. J. Cancer 136 (5) (2015) E290–E300.
[4] A. Temblador, D. Topalis, G. Andrei, R. Snoeck, CRISPR/Cas9 editing of the polyomavirus tumor antigens inhibits Merkel cell carcinoma growth in vitro, Cancers 11 (9) (2019).
[5] J.C. Becker, A. Stang, J.A. DeCaprio, L. Cerroni, C. Lebbe, M. Veness, P. Nghiem, Merkel cell carcinoma, Nat. Rev. Dis. Prim. 3 (2017), 17077.
[6] A.S. Moshiri, R. Doumani, L. Yelistratova, A. Blom, K. Lachance, M.M. Shinohara, M. Delaney, O. Chang, S. McArdle, H. Thomas, M.M. Asgari, M.-L. Huang, S. M. Schwartz, P. Nghiem, Polyomavirus-negative Merkel cell carcinoma: a more aggressive subtype based on analysis of 282 cases using multimodal tumor virus detection, J. Invest. Dermatol. 137 (4) (2017) 819–827.
[7] M. Heath, N. Jaimes, B. Lemos, A. Mostaghimi, L.C. Wang, P.E. Penas, P. Nghiem, Clinical characteristics of Merkel cell carcinoma at diagnosis in 195 patients: the AEIOU features, J. Am. Acad. Dermatol. 58 (3) (2008) 375–381.
[8] Y.D. Tseng, M.H. Nguyen, K. Baker, M. Cook, M. Redman, K. Lachance, S. Bhatia, J. J. Liao, S. Apisarnthanarax, P.T. Nghiem, U. Parvathaneni, Effect of patient immune status on the efficacy of radiation therapy and recurrence-free survival among 805 patients with Merkel cell carcinoma, Int. J. Radiat. Oncol. Biol. Phys. 102 (2) (2018) 330–339.
[9] A. Stang, J.C. Becker, P. Nghiem, J. Ferlay, The association between geographic location and incidence of Merkel cell carcinoma in comparison to melanoma: an international assessment, Eur. J. Cancer 94 (2018) 47–60.
[10] Y. Lee, P. Chao, C. Coomarasamy, J.A. Mathy, Epidemiology and survival of Merkel cell carcinoma in New Zealand: a population-based study between 2000 and 2015 with international comparison, Australas. J. Dermatol. (2019).
[11] S.E. Uitentuis, M.W.J. Louwman, A.C.J. van Akkooi, M. Bekkenk, Treatment and survival of Merkel cell carcinoma since 1993: a population-based cohort study in The Netherlands, J. Am. Acad. Dermatol. (2019).
[12] P.W. Harms, K.L. Harms, P.S. Moore, J.A. DeCaprio, P. Nghiem, M.K.K. Wong, I. Brownell, International Workshop on Merkel Cell Carcinoma Research Working, G., the biology and treatment of Merkel cell carcinoma: current understanding and research priorities, Nat. Rev. Clin. Oncol. (2018).
[13] D. Schadendorf, C. Lebbe, A. Zur Hausen, M.-F. Avril, S. Hariharan, M. Bharmal, J. C. Becker, Merkel cell carcinoma: epidemiology, prognosis, therapy and unmet medical needs, Eur. J. Cancer 71 (2017) 53–69.
[14] I.S. Chan, S. Bhatia, H.L. Kaufman, E.J. Lipson, Immunotherapy for Merkel cell carcinoma: a turning point in patient care, J Immunother Cancer 6 (1) (2018) 23.
[15] M.D.C. Gonzalez-Vela, S. Curiel-Olmo, S. Derdak, S. Beltran, M. Santibanez, N. Martinez, A. Castillo-Trujillo, M. Gut, R. Sanchez-Pacheco, C. Almaraz, L. Cereceda, B. Llombart, A. Agraz-Doblas, J. Revert-Arce, J.A. Lopez Guerrero, M. Mollejo, P.I. Marron, P. Ortiz-Romero, L. Fernandez-Cuesta, I. Varela, I. Gut, L. Cerroni, M.A. Piris, J.P. Vaque, Shared oncogenic pathways implicated in both virus-positive and UV-induced Merkel cell carcinomas, J. Invest. Dermatol. 137 (1) (2017) 197–206.
[16] C. Hafner, R. Houben, A. Baeurle, C. Ritter, D. Schrama, M. Landthaler, J.C. Becker, Activation of the PI3K/AKT pathway in Merkel cell carcinoma, PLoS One 7 (2) (2012), e31255.
[17] V. Nardi, Y. Song, J.A. Santamaria-Barria, A.K. Cosper, Q. Lam, A.C. Faber, G. M. Boland, B.Y. Yeap, K. Bergethon, V.L. Scialabba, H. Tsao, J. Settleman, D. P. Ryan, D.R. Borger, A.K. Bhan, M.P. Hoang, A.J. Iafrate, J.C. Cusack, J. A. Engelman, D. Dias-Santagata, Activation of PI3K signaling in Merkel cell carcinoma, Clin. Cancer Res. 18 (5) (2012) 1227–1236.
[18] Z. Lin, A. McDermott, L. Shao, A. Kannan, M. Morgan, B.C. Stack Jr., M. Moreno, D. A. Davis, L.A. Cornelius, L. Gao, Chronic mTOR activation promotes cell survival in Merkel cell carcinoma, Cancer Lett. 344 (2) (2014) 272–281.
[19] P.W. Harms, P. Vats, M.E. Verhaegen, D.R. Robinson, Y.-M. Wu, S. M. Dhanasekaran, N. Palanisamy, J. Siddiqui, X. Cao, F. Su, R. Wang, H. Xiao, L. P. Kunju, R. Mehra, S.A. Tomlins, D.R. Fullen, C.K. Bichakjian, T.M. Johnson, A. A. Dlugosz, A.M. Chinnaiyan, The distinctive mutational spectra of polyomavirus-negative Merkel cell carcinoma, Cancer Res. 75 (18) (2015) 3720–3727.
[20] A. Kannan, Z. Lin, Q. Shao, S. Zhao, B. Fang, M.A. Moreno, E. Vural, B.C. Stack Jr., J.Y. Suen, K. Kannan, L. Gao, Dual mTOR inhibitor MLN0128 suppresses Merkel cell carcinoma (MCC) xenograft tumor growth, Oncotarget 7 (6) (2016) 6576–6592.
[21] L.M. Ballou, R.Z. Lin, Rapamycin and mTOR kinase inhibitors, J Chem Biol 1 (1–4) (2008) 27–36.
[22] M.C. Mendoza, E.E. Er, J. Blenis, The Ras-ERK and PI3K-mTOR pathways: cross-talk and compensation, Trends Biochem. Sci. 36 (6) (2011) 320–328.
[23] M. Bhat, N. Robichaud, L. Hulea, N. Sonenberg, J. Pelletier, I. Topisirovic, Targeting the translation machinery in cancer, Nat. Rev. Drug Discov. 14 (4) (2015) 261–278.
[24] M. Shuda, H.J. Kwun, H. Feng, Y. Chang, P.S. Moore, Human Merkel cell polyomavirus small T antigen is an oncoprotein targeting the 4E-BP1 translation regulator, J. Clin. Invest. 121 (9) (2011) 3623–3634.
[25] T. Muranen, L.M. Selfors, D.T. Worster, M.P. Iwanicki, L. Song, F.C. Morales, S. Gao, G.B. Mills, J.S. Brugge, Inhibition of PI3K/mTOR leads to adaptive resistance in matrix-attached cancer cells, Cancer Cell 21 (2) (2012) 227–239.
[26] A. Carracedo, L. Ma, J. Teruya-Feldstein, F. Rojo, L. Salmena, A. Alimonti, A. Egia, A.T. Sasaki, G. Thomas, S.C. Kozma, A. Papa, C. Nardella, L.C. Cantley, J. Baselga, P.P. Pandolfi, Inhibition of mTORC1 leads to MAPK pathway activation through a PI3K-dependent feedback loop in human cancer, J. Clin. Invest. 118 (9) (2008) 3065–3074.
[27] J.J. Caumanns, A. van Wijngaarden, A. Kol, G.J. Meersma, M. Jalving, R. Bernards, A.G.J. van der Zee, G.B.A. Wisman, S. de Jong, Low-dose triple drug combination

targeting the PI3K/AKT/mTOR pathway and the MAPK pathway is an effective approach in ovarian clear cell carcinoma, Cancer Lett. 461 (2019) 102–111.
[28] T. Iwasaki, K. Hayashi, M. Matsushita, D. Nonaka, K. Kohashi, S. Kuwamoto, Y. Umekita, Y. Oda, Merkel cell polyomavirus-negative Merkel cell carcinoma is associated with JAK-STAT and MEK-ERK pathway activation, Cancer Sci. (2021).
[29] C.J. Caunt, M.J. Sale, P.D. Smith, S.J. Cook, MEK1 and MEK2 inhibitors and cancer therapy: the long and winding road, Nat. Rev. Cancer 15 (10) (2015) 577–592.
[30] J.C. Chamcheu, T. Roy, M.B. Uddin, S. Banang-Mbeumi, R.-C.N. Chamcheu, A. L. Walker, Y.-Y. Liu, S. Huang, Role and therapeutic targeting of the PI3K/Akt/mTOR signaling pathway in skin cancer: a Review of current status and future trends on natural and synthetic agents therapy, Cells 8 (8) (2019).
[31] T.C. Chou, P. Talalay, Quantitative analysis of dose-effect relationships: the combined effects of multiple drugs or enzyme inhibitors, Adv. Enzym. Regul. 22 (1984) 27–55.
[32] T.-C. Chou, Theoretical basis, experimental design, and computerized simulation of synergism and antagonism in drug combination studies, Pharmacol. Rev. 58 (3) (2006) 621–681.
[33] T.-C. Chou, Drug combination studies and their synergy quantification using the Chou-Talalay method, Cancer Res. 70 (2) (2010) 440–446.
[34] K.G. Paulson, S.Y. Park, N.A. Vandeven, K. Lachance, H. Thomas, A.G. Chapuis, K. L. Harms, J.A. Thompson, S. Bhatia, A. Stang, P. Nghiem, Merkel cell carcinoma: current US incidence and projected increases based on changing demographics, J. Am. Acad. Dermatol. 78 (3) (2018) 457–463, e2.
[35] S.P. D'Angelo, J. Russell, C. Lebbe, B. Chmielowski, T. Gambichler, J.-J. Grob, F. Kiecker, G. Rabinowits, P. Terheyden, I. Zwiener, M. Bajars, M. Hennessy, H. L. Kaufman, Efficacy and safety of first-line avelumab treatment in patients with stage IV metastatic Merkel cell carcinoma: a preplanned interim analysis of a clinical trial, JAMA Oncol. 4 (9) (2018), e180077.
[36] P. Nghiem, S.Y. Park, Less toxic, more effective treatment-A win-win for patients with Merkel cell carcinoma, JAMA Dermatol. (2019).
[37] R. Bayat Mokhtari, T.S. Homayouni, N. Baluch, E. Morgatskaya, S. Kumar, B. Das, H. Yeger, Combination therapy in combating cancer, Oncotarget 8 (23) (2017) 38022–38043.
[38] H. Sato, H. Yamamoto, M. Sakaguchi, K. Shien, S. Tomida, T. Shien, H. Ikeda, M. Hatono, H. Torigoe, K. Namba, T. Yoshioka, E. Kurihara, Y. Ogoshi, Y. Takahashi, J. Soh, S. Toyooka, Combined inhibition of MEK and PI3K pathways overcomes acquired resistance to EGFR-TKIs in non-small cell lung cancer, Cancer Sci. 109 (10) (2018) 3183–3196.
[39] R. Houben, M. Shuda, R. Weinkam, D. Schrama, H. Feng, Y. Chang, P.S. Moore, J. C. Becker, Merkel cell polyomavirus-infected Merkel cell carcinoma cells require expression of viral T antigens, J. Virol. 84 (14) (2010) 7064–7072.
[40] A.M. Schram, L. Gandhi, M.M. Mita, L. Damstrup, F. Campana, M. Hidalgo, E. Grande, D.M. Hyman, R.S. Heist, A phase Ib dose-escalation and expansion study of the oral MEK inhibitor pimasertib and PI3K/MTOR inhibitor voxtalisib in patients with advanced solid tumours, Br. J. Cancer 119 (12) (2018) 1471–1476.
[41] F.J. Esteva, V.M. Hubbard-Lucey, J. Tang, L. Pusztai, Immunotherapy and targeted therapy combinations in metastatic breast cancer, Lancet Oncol. 20 (3) (2019) e175–e186.